ELEMENTA
Science of the Anthropocene

Hrycyna, E, et al. 2022. Satellite observations of NO_2 indicate legacy impacts of redlining in U.S. Midwestern cities. *Elem Sci Anth*, 10: 1. DOI: https://doi.org/10.1525/elementa.2022.00027

RESEARCH ARTICLE

Satellite observations of NO_2 indicate legacy impacts of redlining in U.S. Midwestern cities

Elizabeth Hrycyna[1], Jennings G. A. Mergenthal[1], Saiido Noor[1], and Mary A. Heskel[1,*]

Redlining was a practice of financial discrimination in the mid-20th century in which banks refused loans or increased interest rates based on the grade of an applicant's neighborhood as designated by the federally sponsored Home Owner's Lending Commission (HOLC). The HOLC primarily graded neighborhoods from "A" (best) to "D" (hazardous) based on characteristics including the racial demographics and economic status of the residents, with neighborhoods with higher percentages of non-white and/or recent immigrant residents given lower grades; this and similar discriminatory practices can be traced to modern-day economic and environmental inequalities between neighborhoods. The legacy of redlining and related housing discrimination on modern-day urban air quality, which presents a significant threat to public health, remains an important issue in addressing environmental injustice in U.S. cities. In our study, we used remotely sensed estimates of the air pollutant nitrogen dioxide (NO_2) collected with the TROPOMI satellite sensor, and shapefiles of redlined neighborhoods, to determine whether air quality varies among historic HOLC grades in 11 U.S. Midwestern metropolitan areas. This approach allowed us to test these tools for within-city analysis of NO_2 for which high spatial and temporal resolution measurements are not often available, despite their importance for monitoring impacts on human health. We found that NO_2 levels were as much as 16% higher in neighborhoods that were graded "D" compared to those graded "A" (as in Chicago), with the mean difference across all cities an increase of 7.3% $\pm$ 5.9%. These results present evidence of persistent modern-day inequality in urban air quality associated with historic discriminatory policies and should be used as an argument for government action improving air quality in neighborhoods that were poorly graded by the HOLC.

Keywords: Redlining, Urban air quality, Nitrogen dioxide, Urban ecology, HOLC, TROPOMI

Introduction

Urban housing in the United States is often highly segregated by race and socioeconomic status (Rothstein, 2017). In part, these patterns can be explained by (1) legacies of government policies and practices that prevented non-white and/or immigrant residents from moving into certain neighborhoods through explicit or indirect economic and legal barriers, and (2) active and passive steps made by municipal to federal governments that devalued and neglected neighborhoods composed primarily of residents of color (Woods, 2012; Fishback et al., 2021; Winling and Michney, 2021). "Redlining" was one such practice that categorized neighborhoods in metropolitan areas by assessed risk for home loans (Zenou and Boccard, 2000; Rothstein, 2017; Winling and Michney, 2021). The federally organized and supported Home Owner's Lending Commission (HOLC) that established this systematic neighborhood categorization was a government program, initiated and funded to increase homeownership rates and economically support homeowners threatened by foreclosure during and after the Great Depression (Rothstein, 2017; Winling and Michney, 2021). The HOLC categorized neighborhoods into 1 of 4 grades. In ascending order of assessed "quality," they were D, "Hazardous," outlined in red or "redlined" (which also refers to the overall practice); C, "Definitely declining," outlined in yellow; B, "Still desirable," outlined in blue; and A, "Best" outlined in green or "greenlined" (Woods, 2012; Rothstein, 2017). Assessed risk for loans was based not only on the quality of the properties but on the racial, immigrant, and socioeconomic makeup of the neighborhood (Zenou and Boccard, 2000; Winling and Michney, 2021). The presence of non-white, immigrant, and low-income residents often settled a neighborhood in the high-risk category according to the HOLC, which meant loans were denied to residents or offered at higher interest rates (Woods, 2012; Park and Quercia, 2020; Fishback et al., 2021). Residents of so-called "redlined" neighborhoods were therefore less likely to recover financially from the Great Depression, less likely to benefit from intergenerational financial benefits of homeownership, and were more likely to be

[1] Department of Biology, Macalester College, Saint Paul, MN, USA

* Corresponding author:
Email: mheskel@macalester.edu

Downloaded from http://online.ucpress.edu/elementa/article-pdf/10/1/00027/735603/elementa.2022.00027.pdf by guest on 15 August 2022

economically limited to areas in which resources were steadily declining due to decades of underinvestment and neglect at the municipal, state, and federal levels (Park and Quercia, 2020; Fishback et al., 2021).

While the explicit practice of redlining was made illegal over 50 years ago in 1968 with the establishment of the Fair Housing Act, its lasting impacts can be mapped to current social, economic, demographic, and environmental inequalities in communities and cities today (Woods, 2012; Rothstein, 2017; Park and Quercia, 2020). Redlined neighborhoods are still home to disproportionately low-income and non-white residents, while greenlined neighborhoods are broadly composed of higher income and predominantly white residents (Zenou and Boccard, 2000; Mitchell and Franco, 2018). It should also be noted that the Federal Housing Administration and its exclusionary practice of not insuring mortgages for residents of Black neighborhoods, which pre-dated HOLC practices, also contributed substantially to historic and ongoing inequality of homeownership (Fishback et al., 2021). An analysis of 10 major cities found significantly higher rates of cancer, asthma, poor mental health, and lack of health insurance in lower graded urban zones (Nardone et al., 2020c). Recently published studies using remotely sensed and ground-based measurements identified clear environmental differences between redlined and greenlined areas, including higher surface temperatures, more impervious surface cover, and lower canopy cover and green space in redlined neighborhoods (Grove et al., 2018; Hoffman et al., 2020; Moxley and Fischer, 2020; Wilson, 2020; Locke et al., 2021). Urban air quality, which is important to public health and disproportionally burdens neighborhoods with non-white and low-income residents (Miranda et al., 2011; Clark et al., 2014; Hajat et al., 2015; Demetillo et al., 2020; Liu et al., 2021), is not always studied in relation to the historic geographies demarcated via redlining, though there are recent analyses that examine these patterns (Namin et al., 2020; Nardone et al., 2020b). Inequities in air quality and how communities of color are disproportionately impacted by air pollution is observed in both urban and rural regions, as well as across different income levels (Tessum et al., 2019; Tessum et al., 2021). These trends are so persistent that air quality continued to be worse in non-white communities even during lockdown periods early in the COVID-19 pandemic (Kerr et al., 2021). In our study, we seek to address these persistent environmental justice issues in U.S. urban areas and apply remote-sensing methods to examine whether historic policies and their indirect and direct impacts relate to urban air quality in the present day.

Urban air quality has been explicitly connected to patterns of redlining in a few recent studies (Namin et al., 2020; Gonzalez et al., 2022; Lane et al., 2022), and a growing body of literature has connected these historic policies with increased prevalence of lower health outcomes (described and referenced below). Air quality, as estimated through measures of airborne carcinogens, has been shown to be worse in communities of color and low-income neighborhoods and linked to higher rates of asthma, multiple types of cancer, heat-related illnesses, and respiratory and heart disease in residents of these neighborhoods (Morello-Frosch and Jesdale, 2006; Krieger et al., 2020a; Nardone et al., 2020a; Li et al., 2021). Low birthweight, preterm birth, and allergies are also linked to poor urban air quality (Rumchev et al., 2007; Miranda et al., 2011; Kelly and Fussell, 2015; Nardone et al., 2020a; Krieger et al., 2020b).

Over 3,000 different air pollutants have been identified globally with only a fraction of those investigated for health effects and even fewer monitored in urban areas (Fenger, 2002). The Clean Air Acts of 1970 and 1977 include 6 air pollutants in a category called "Criteria Air Pollutants," which are monitored and regulated nationally, and often occur at high concentrations (Fenger, 2002; Miranda et al., 2011). This category includes the pollutant we focus on for this study—nitrogen dioxide (NO_2)—as well as carbon monoxide (CO), ozone (O_3), particulate matter, lead, and sulfur dioxide. It has been estimated that more than 50% of the U.S. population lives in air that exceeds federal standards for at least one major air pollutant, making air quality of immediate importance in our rapidly urbanizing world (D'Amato et al., 2010); however, more recent regional legislative policies and air quality regulations may have shifted this estimate to a lower coverage.

A recent study identified that Black and non-white Hispanic communities are more likely to shoulder a disproportionately higher air "pollution burden" than white communities, despite contributing significantly less to pollution production through consumption patterns (Tessum et al., 2019). These results are further supported by recent studies focusing on pollutant exposure differences among HOLC neighborhoods (Gonzalez et al., 2022; Lane et al., 2022). Collectively, recent research emphasizes the important need to prioritize public health and environmental equity across the United States to identify and correct historic and ongoing harms.

However, mapping environmental disparities in air quality can be challenging to track in real time and at high resolution. Efforts to accurately measure patterns and sources of air pollution are limited by the spatial and temporal resolution of air quality monitoring data. Most publicly available continuously monitored air quality datasets (i.e., the U.S. Environmental Protection Agency's [EPA's] National Emissions Inventory) often only include one or two sampling locations per city. Namin et al. (2020) used data from the EPA's National Air Toxic Assessment (NATA) to assess variation of airborne carcinogens between different HOLC neighborhoods and found a correlation between air pollution and HOLC grade, with increasing carcinogens detected in lower graded neighborhoods. NATA provides census-tract level data but is only available as single data point "snapshots" every few years (http://www.epa.gov/national-air-toxics-assessment), thus the lower temporal resolution that may not catch seasonal or year-to-year variability.

To address the discrepancy in resolution, satellite data show promise in examining the spatial and temporal variation of other environmental factors between HOLC neighborhoods *within* a city, in addition to *across* cities. Recent examples of this application, including both

Downloaded from http://online.ucpress.edu/elementa/article-pdf/10/1/00027/735603/elementa.2022.00027.pdf by guest on 15 August 2022

Table 1. Demographic and geographic data for the 11 sampled cities

City	State	Population	Pop. Density (Individuals mi^{-2})	Area (mi^2)	% A	% B	% C	% D
St. Paul	MN	308,096	5,484	134.6	13	28	31	27
Minneapolis	MN	429,606	7,088	139.8	14	39	30	17
Cleveland	OH	381,009	5,107	201.2	11	23	47	18
Milwaukee	WI	590,157	6,188	248.9	8	19	49	24
Omaha	NE	478,192	3,218	329.2	18	52	25	5
Detroit	MI	670,031	5,144	359.4	6	14	51	28
Wichita	KS	389,938	2,400	412.6	15	8	13	64
Columbus	OH	898,553	2,172	562.5	15	29	39	18
Chicago	IL	2,693,976	11,842	589.6	4	17	50	29
Indianapolis	IN	876,384	2,270	936.1	5	9	59	27
Greater Kansas City	MO, KS	1,165,358	1,314	1,139	5	9	33	52

Population size (from 2019), density (from 2010), and spatial area of city (from 2019) for each of the sampled metropolitan areas included in our study, from the U.S. Census Bureau. The percentage of the total HOLC (Home Owner's Loan Commission) classified city area (derived from the entire area of the original HOLC map) that was categorized into neighborhood designations A, B, C, and D is shown for each city, based on spatial information obtained from *Mapping Inequality* (Nelson et al., 2021).

a smaller study of 3 cities and a larger analysis of 108 cities using satellite estimates, confirm that redlined neighborhoods experience significantly higher land surface temperatures (Hoffman et al., 2020; Wilson, 2020). The recent 2017 launch of the Copernicus satellite Sentinel-5 carrying the tropospheric monitoring instrument (TROPOMI) created a database of high-resolution, near-continuously monitored satellite-derived data of the pollutant NO_2, among others, that can be applied to analyze spatial variation across the globe. Further, increased temporal resolution allows for examinations of intra- and interannual comparisons within and across sites to answer questions about human, industrial, and seasonally mediated shifts in air quality (Goldberg et al., 2019; Goldberg et al., 2021). Recently, these data were applied to address changes due to the disruptions caused by the COVID-19 pandemic (Kerr et al., 2021; Jing and Goldberg, 2022; Tzortziou et al., 2022) and urban inequities (Demetillo et al., 2020; Anenberg et al., 2022). These data create new opportunities for higher resolution air quality monitoring in space and time, within and across cities and regions, providing a robust tool for examining current environmental variation in atmospheric pollutant loads.

Our study seeks to apply these high-resolution data to address how (1) U.S. Midwestern cities vary in the levels of a noxious air pollutant (NO_2) and (2) how this pollutant varies within these cities among historic HOLC neighborhood grades. We do this using satellite-collected TROPOMI data of NO_2 for the entire calendar year of 2019, prior to COVID-influenced shifts in traffic and industry during 2020, which have altered air quality in urban U.S. areas (Kerr et al., 2021; Cooper et al., 2022; Jing and Goldberg, 2022; Tzortziou et al., 2022). We hypothesized that, despite a half century since the elimination of codified neighborhood categorization via HOLC, the historic legacies of redlining and associated policies and practices would still be detected in these data, with higher air pollutant load in red and yellow neighborhoods compared to blue and green neighborhoods. Environmental inequities, detected at the ground or from space, demand close monitoring and immediate resolution to protect residents from current pollutants and the compounded impacts of climate change in these cities.

Methods

City selection

The top 10 most populated metropolitan areas in the Midwest were selected for inclusion in our analysis. Cities with populations at or exceeding 350,000 residents were selected with the aim of including cities that would provide increased air pollution variation due to greater intra-city urbanization and population density patterns. The selected cities are in decreasing population size, Chicago, IL; Columbus, OH; Indianapolis, IN; Detroit, MI; Greater Kansas City metropolitan area, MO and KS; Milwaukee, WI; Omaha, NE; Minneapolis, MN; Wichita, KS; and Cleveland, OH (**Table 1**). The Greater Kansas City metropolitan area combines Kansas City, MO, and Kansas City, KS. This combination was necessary because the redlining map available through Mapping Inequality (see below) covered Greater Kansas City and was not divided by state. St. Paul was included as the 11th city in the analysis because although it has a population of less than 350,000 residents, it is the location of our home institution, Macalester College. Population size and geographic area reported represent 2019 data and the population density represent 2010 data, all collected from the U.S. Census Bureau.

Chicago is by far the most populous city included in this study with approximately 2 million residents as of 2019, while all other cities fall below the 900,000

Downloaded from http://online.ucpress.edu/elementa/article-pdf/10/1/00027/735603/elementa.2022.00027.pdf by guest on 15 August 2022

residents mark (**Table 1**). Wichita, KS; Cleveland, OH; and St. Paul, MN, are the least populated cities at 380,000 residents or fewer each (**Table 1**). Cities vary widely in population density and spatial area, providing axes of variation to interpret the results of air quality differences and impacts on the population (**Table 1**).

HOLC maps

Historic maps commissioned and created by the HOLC were made available through the University of Richmond's publicly accessible website *Mapping Inequality* (Nelson et al., 2021). These maps are composite images of multiple historical redlining maps collected and georectified from various years between 1936 and 1940 (or year not indicated). Percentages of spatial area covered by different HOLC zones for each city were available through the website and used in our analysis (see **Table 1**). The area of the redlining maps may not exactly correspond to the current geographic area of their corresponding cities since individual cities may have expanded spatially since the redlining maps were made in the mid-1900s. The percentages of each city that fall under each HOLC grade are percentages of the entire redlining map and not the modern city area (**Table 1**). ArcGIS shapefiles of the maps of each city of interest were downloaded from *Mapping Inequality* and uploaded to Google Earth Engine for our air quality analyses.

Estimates of urban air quality using remote sensing approaches

The Copernicus satellite Sentinel-5 Precursor (Sentinel-5P) is an Earth-observing satellite carrying the TROPOMI which monitors atmospheric air quality and ultraviolet radiation, and contributes to climate monitoring (https://sentinel.esa.int/web/sentinel/missions/sentinel-5p). The satellite is designed for a 7-year life span and was launched in October 2017. Sentinel-5P collects data for near real-time atmospheric columnar densities of NO_2. The data became publicly available in July 2018, 8 months postlaunch, and has been continuously updated up to the present. The NO_2 data collected via the TROPOMI sensor is available for direct import into the Google Earth Engine where it can be visualized and downloaded (Gorelick et al., 2017). Nitrogen dioxide was selected for analysis as it is one of the 6 EPA Criteria Air Pollutants, given its impact on human health. The spatial resolution is 3.5×7 km^2 for NO_2, which is a resolution that lends itself effectively for intra-urban studies of air quality. TROPOMI is a polar-orbiting satellite, measuring tropospheric column gasses during its one-a-day overpass time (approximately early afternoon). Given the conditions during this time point, there may be measurements that are not accurately representative of the average daily pollutant load. It should also be mentioned that these data are not a stand in for air quality on the ground experienced by city residents, but there is promise in linking these for more appropriate estimates (Demetillo et al., 2020; Kerr et al., 2021).

The Earth Engine Code Editor (EECodeEditor) administered by Google Earth is an online programming tool to manipulate geospatial data and remotely sensed satellite imagery and information (Gorelick et al., 2017). We imported the publicly accessible HOLC map shapefiles from *Mapping Inequality* (Nelson et al., 2021) to the EECodeEditor to visualize the historic boundaries of red, yellow, blue, and green (i.e., D, C, B, A) neighborhoods on the current landscapes of the metropolitan areas as they appear in the current day. These shapefiles for each city of interest were imported as a FeatureCollection in the EECodeEditor. The HOLC neighborhood polygons vary in shape and can have a large range of sizes and areas even within a single city. To enhance the representation of the NO_2 data and minimize oversampling of pixels, we merged adjacent, contiguous polygons of the same HOLC grade by dissolving their shared boundaries to produce new, larger polygon of that grade (Table S1). For all analyses, we present data using these larger, merged polygons.

We imported Sentinel-5P data of the tropospheric level column NO_2 density (mol m^{-2}) between the surface and the top of the troposphere into the EECodeEditor within the bounds of each city. Data were imported for the time period of January 1, 2019, to January 1, 2020. Data from the year 2020 was excluded due to potential abnormal variation in fossil fuel emissions and resulting pollutant levels caused by changes in human industrial and transportation activity triggered by the COVID-19 pandemic (Le Quéré et al., 2020; Tzortziou et al., 2022; Jing and Goldberg, 2022). We imported the offline Sentinel-5P Level 3 NO_2 data product, which filters pixels with a QA >0.75. The NO_2 values from TROPOMI imagery within this time period were bounded and averaged spatially by the larger, merged HOLC polygons (described in the previous paragraph). Mean value calculations were area-weighted for polygons that contain more than one full pixel, and/or is partially (>0.5% within the polygon) covered by a pixel. The centroid of the pixel is not required to fall inside the polygon to be included in this calculation. The date and time stamp for each satellite image was also extracted, as well as the number of pixels per polygon, which is reported in Table S2.

The data for our analyses included the HOLC neighborhood grade of the merged neighborhood polygon, the mean air pollutant density value for the merged HOLC neighborhood, the area of each merged neighborhood polygon (Table S1), the number of pixels included in the polygon that were used to calculate the mean daily value (Table S2), and the date and time of the satellite image from which each data point was collected for all of 2019. Knowing that many cities contained smaller neighborhoods that were either noncontiguous with other same-grade neighborhoods (so they weren't merged to make a larger polygon) or when merged were still very small in area, we only analyzed data for merged polygons which were greater than 2 km^2. This filtering by area allowed us to reduce overrepresenting small area neighborhoods in our analyses which limits oversampling of the same pixel. While this approach has the potential to remove some small, isolated, high-emitting small neighborhoods, we believe it allows for greater alignment of pixel area and minimizes bias introduced by these potential neighborhoods. Sample size of all NO_2 observations for all HOLC grades in each city are reported in Table S3.

Downloaded from http://online.ucpress.edu/elementa/article-pdf/10/1/00027/735603/elementa.2022.00027.pdf by guest on 15 August 2022

All NO_2 data were converted from mol m^{-2} into Dobson Units, where 1 DU = 2.69×10^{16} molecules cm^{-2}.

Data analyses

All statistical analysis and graphical plots were created in RStudio (version 1.2.5032), using the programming language R (version 3.6.3) (R Core Team, 2021). Negative NO_2 values which indicated an error in the data collection were excluded from analysis, as were NA values. We conducted a power analysis to determine whether our sampling design met criteria to determine differences between the HOLC-graded neighborhoods. Using the *pwr* package in R (Champley, 2020) and setting our effect size to 0.10 based on our assumption that satellite-derived air pollutant detection may not yield large value differences among areas in urban regions (compared to the large effect sizes we might assume when comparing across different land use types, for instance), we found a minimum sample size of $n = 274$ to detect significance among 4 groups. Table S3 shows the sample sizes for our analyzed data, note that only 9 of 44 HOLC grades across all cities' categories contained less than the suggested sample size from our power analysis. NO_2 followed a natural-log distribution and was natural-log-transformed for all statistical analyses, though plots show untransformed data for clarity.

To assess the influence of historic redlining neighborhood categorization on NO_2 in our all-city dataset analysis, we employed a linear mixed effects model, where NO_2 was set to vary by HOLC grade as a fixed effect (meaning that it was analyzed as the driver variable influencing the outcome) and city was set as a random effect (meaning it is likely to contribute to variance but is not the focused driver of variation in our study). Considering all cities' data in the two-way ANOVA, we evaluated how the city and HOLC grades influenced the outcomes together. Tukey HSD post hoc analysis tests were performed on the two-way ANOVA results to determine significance among HOLC grades and cities. One-way ANOVA and Tukey HSD tests were performed within each city, considering each cities' data independently, and significant results are reported. We used R packages *multcomp*, *emmeans*, *lme4*, and the *tidy* packages to conduct our data and statistical analyses (Hothorn et al., 2008; Wickham, 2021; Lenth, 2022).

We were also interested in assessing how coarse city demographic and geographic variables might be used to explain variance in the observed NO_2 values collected from TROPOMI. To do this, we used a linear mixed-model regression to examine the response of observed NO_2 across cities to the following variables: population size, population density, and geographic area of the city, with city included as a random effect. Each variable was assessed independently to compare the relative explanatory strength of the models. We report the R^2 and P values of each linear model.

Results

Collectively, our results point to varied NO_2 emissions in Midwestern cities that are often related to both the city itself and the HOLC grades within a city. Analyses reveal the likelihood that legacy impacts of redlining are present as observed through the often-worse air quality estimates in D-grade neighborhoods, supported by other satellite-based estimates of common pollutants that have hazardous impacts on the respiratory health of residents (Demetillo et al., 2020; Kerr et al., 2021). Higher NO_2 levels are related to D-graded neighborhoods in many of the most populous Midwestern cities. Coarse variables of city population size and density also show some positive relationships with NO_2 levels.

HOLC grades vary among and within cities for NO_2

Considering the entire dataset of all Midwestern cities, NO_2 varies significantly between HOLC grades (**Figure 1**; **Table 2**). A-graded neighborhoods showed the lowest NO_2 levels, followed by B, and then finally D neighborhoods, in which the highest mean values were observed (**Figure 1**). There were no significant differences among values of C neighborhoods and values of both B and D values (**Figure 1**). The differences between HOLC grades were highly significant ($P < 0.001$). All estimates of TROPOMI-derived values of NO_2 ranged between approximately 6×10^{-5} and 1.35 DU, while the differences between the HOLC grades' mean NO_2 did not exceed 0.012 DU. The largest difference in values considering the all-city data is observed between D and A grades, approximately 0.012 DU greater NO_2 in D-grade neighborhoods. For context, the interquartile range of the all cities data is 0.096, and the interquartile ranges for each HOLC grade (A, B, C, D) are 0.087, 0.095, 0.095, and 0.101, respectively.

Individual city analyses found NO_2 is significantly different among HOLC grades in about half of the sampled metropolitan areas (5 of 11). NO_2 did not significantly vary between any HOLC grades in Columbus, Detroit, Minneapolis, Omaha, St. Paul, and Wichita (**Figure 2**; **Table 2**). Four of those cities had sample size less than 274 in at least one neighborhood grade (Table S3), though there was no absolute trend connecting high or low sample size cities with significance. Of the 5 cities where significant differences among HOLC neighborhoods were detected, D neighborhoods had the highest average NO_2 values (**Figure 2**, **Table 2**). Specifically, in Chicago, Cleveland, Greater Kansas City, and Indianapolis, D and A neighborhoods were significantly different from each other with A grades showing the lowest values of NO_2 and D the highest (**Figure 2**). In Milwaukee, only D and B grades were significantly different, with B having the lowest mean values (**Figure 2**; **Table 2**). Chicago, Indianapolis, and Greater Kansas City showed the most distinct differences between HOLC grades of A and D, and the highest percent increases in NO_2 values at 16.2%, 13.0%, and 15.4%, respectively (**Figure 2**). Chicago anchors this trend with the greatest absolute difference in mean values of NO_2 between D and A neighborhoods at 0.0328 DU (**Figure 2**), for context the interquartile range considering data from all HOLC grades in Chicago is 0.159. Chicago also reports the highest overall values (in DU) of NO_2 across the study for each

Downloaded from http://online.ucpress.edu/elementa/article-pdf/10/1/00027/735603/elementa.2022.00027.pdf by guest on 15 August 2022

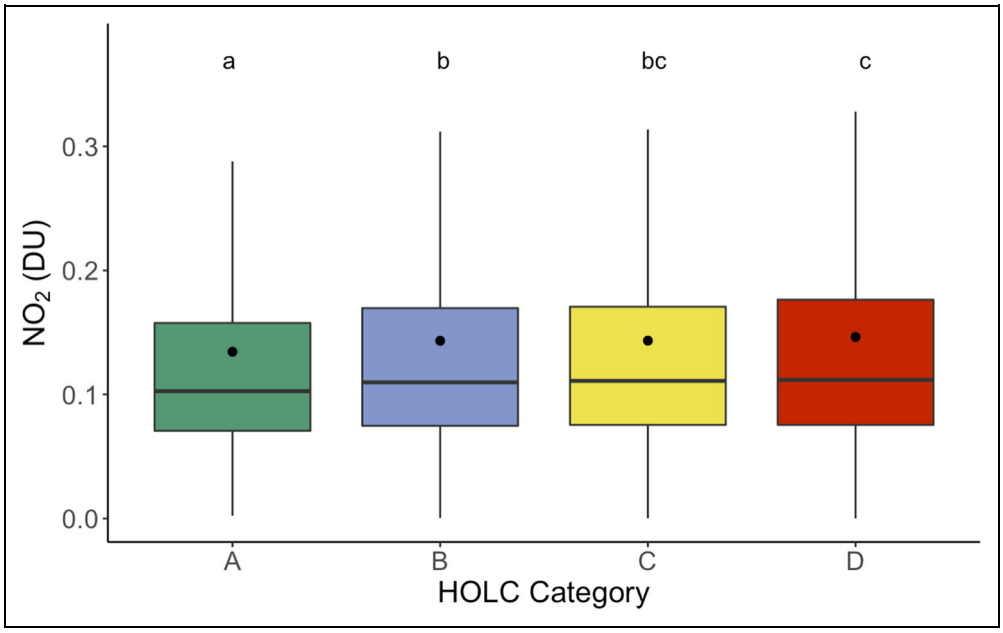

Figure 1. Atmospheric NO_2 levels by HOLC neighborhood across all cities. NO_2 values of all cities for the year 2019, reported in Dobson Units (DU), of HOLC-graded (Home Owner's Loan Commission, which evaluated "risk" for mortgage lenders) neighborhoods (A–D) were compared via analysis of variance (ANOVA; total $n = 14{,}576$). Mean annual values of each HOLC neighborhood category for all cities are: A = 0.134 ± 0.113, B = 0.143 ± 0.116, C = 0.143 ± 0.113, D = 0.146 ± 0.115. Boxplots show the mean (black point), median (horizontal line within box), the 25th and 75th percentiles of the data (upper and lower hinges of the box), and the largest and smallest values within 1.5 times the interquartile range above the 75th and below the 25th percentiles (whiskers extending from box), respectively, for each HOLC-graded neighborhood. Lower-case letters above boxplots indicate significant differences among neighborhood grades according to ANOVA: boxplots annotated with the same letters are not different, whereas boxplots that have unshared, different letters are significantly different from each other based on $P < 0.05$. For instance, in this figure, "A" neighborhood values differ from "B," "C," and "D" neighborhood values (where notation of a ≠ b or c); however, the "C" neighborhood boxplot, annotated with "bc" above it is not different than "B" or "D" neighborhood values, as they are represented by either "b" or "c."

of the neighborhood categories (followed by Detroit), roughly double the estimated values of NO_2 of cities such as Cleveland, Columbus, Milwaukee, and Minneapolis, and triple the estimates for Wichita.

Relating population size, population density, and city area to pollutant levels

The trends in NO_2 found clear differences among HOLC grades only in some of the cities, so we further assessed additional urban demographic and geographic variables that might influence the observed relationships. To do this, we focused on estimates of population size and density, and geographic area. We acknowledge the coarseness of these metrics to compare cities that can be incredibly diverse in their geographies, climates, and industrial and developmental histories, but these metrics may also provide insight into broad controls on NO_2 dynamics across the urban Midwest. Metropolitan population size and density correspond positively but with low predictive power to NO_2 values (**Table 3**). Chicago's population is more than double the size of all other cities included in our study and its population density is 1.5× greater (**Table 1**) and also has higher NO_2 than any other city (Tukey HSD indicates $P < 0.0001$ in all-city analysis). Metropolitan area does not exhibit a clear predictive relationship to NO_2 values among all cities (**Table 3**).

Discussion

Redlining and associated discriminatory practices, whose impacts have been sustained and potentially intensified through direct policies (i.e., highway construction), development patterns (i.e., proximity to industrial activity and pollution), inequitable private lending practices and devalued properties, and political divestment driven by direct and indirect impacts of systemic racism, are observed to relate to modern day air quality in many large Midwestern cities as measured via satellite imagery. HOLC-designated D neighborhoods experience a mean increase in values of NO_2 of 7.3% ± 5.9% compared to A neighborhoods, revealing a legacy of redlining in current day urban air quality. However, a large range of variation is evident among the cities in our study: mean city values ranging from a minimal change of –2.4% in St. Paul to a substantial increase of +16.2% in Chicago. Our study demonstrates the potential of using TROPOMI satellite data to monitor NO_2 levels at high resolution in intra- and inter-urban settings to examine environmental inequities, and we encourage higher resolution, ground-based methods to further identify these persistent inequities.

Downloaded from http://online.ucpress.edu/elementa/article-pdf/10/1/00027/735603/elementa.2022.00027.pdf by guest on 15 August 2022

Table 2. ANOVA results for all-city analysis and of individual cities

Variable	*P* Value	*F* Statistic
HOLC grade	***	43.63
City	***	1,025
HOLC grade × City	***	2.685
City	***P* Value**	***F* Statistic**
Columbus	0.071	2.3
Indianapolis	***	6.4
Chicago	***	29
Wichita	0.084	3.0
Cleveland	***	12
Greater Kansas City	***	8.1
Omaha	0.27	1.3
Detroit	0.14	1.8
Minneapolis	0.070	2.4
St. Paul	0.82	0.31
Milwaukee	*	3.0

The top section shows statistical results of all-city data of NO_2 variation by HOLC (Home Owner's Loan Commission) grade (A–D; $df = 3$), City ($df = 10$), and their interaction (HOLC grade × City, $df = 28$). Differences among HOLC grades are also indicated in **Figure 1**. The bottom section of the table shows results of how NO_2 varies by HOLC (Home Owner's Loan Commission) grade (A–D) for each individual city. We report *P* values and *F* statistic values; statistical significance is reported according to $P < 0.05$ (*) and $P < 0.001$ (***) and nonsignificant tests are indicated with their calculated *P* value. Results of within-city statistical variation by HOLC grade ($df = 3$), as calculated by Tukey HSD post hoc analysis is indicated in **Figure 2**, where shared letters indicate statistical similarities, and different letters indicate significant differences across grades.

Highest burden of NO_2 in D-grade neighborhoods

Nitrogen dioxide data, as collected from the global-monitoring TROPOMI satellite sensor, show promise for measuring intraurban, neighborhood-level differences (Goldberg et al., 2019; Demetillo et al., 2020; Kerr et al., 2021; Cooper et al., 2022). This tool allows us to examine air quality in areas that may have previously been underrepresented in monitoring projects due to lack of resources, including historically redlined neighborhoods. NO_2 is among the most abundant outdoor air pollutants in urban areas (D'Amato et al., 2010) and is associated with increased risk of asthma, stroke, hospitalization for respiratory and cardiac issues, and susceptibility to respiratory infections (Kelly and Fussell, 2015). Anenberg et al. (2022) shows that although urban levels of NO_2 have been decreasing over the past few decades, current levels in high-income countries such as the United States still contribute significantly to prevalence of pediatric asthma, and even moderate declines in urban NO_2 levels can decrease this burden. Our findings show large within-HOLC-grade variation, which indicates other influences on NO_2, including time, day of the week, and climate (Goldberg et al., 2021). While the magnitude of the HOLC-grade variation may seem small, we believe these significant differences point to important trends in inequities of air quality burdens that necessitate ground-based quantification and signify potential exposure disparities that relate to health.

NO_2 from human activity mostly originates from fossil fuel combustion (Fenger, 2002), though recent studies have identified agriculture as a major emitter of NO_2 with influences on public health (Clark et al., 2019; Hill et al., 2019; Goldberg et al., 2021). In the U.S. Midwest, even the largest metropolitan areas are rarely far from intensive, industrial farming of corn and soy, so this agricultural contribution may have more influence in Midwestern versus coastal population centers (Hill et al., 2019). However, given the decay gradients of NO_2 from pollutant sources, the agricultural signal may not extend to urban regions in a significant manner; future examinations of urban-to-rural gradients could address these varied contributions (Demetillo et al., 2020). Our data does show higher absolute values of NO_2 in Chicago and Detroit, nearly triple those observed in Wichita, suggesting diverse influences of geography, climate, and industrial histories. It should be noted that NO_2 is not directly emitted from fuel combustion, rather it forms from the oxidation of nitric oxide (NO), which is produced from incomplete combustion of fuels (Fenger, 2002). However, since this reaction occurs rapidly, NO_2 is formed close to the point source of NO pollution, and thus still highly correlates with areas of high fossil fuel emissions (Fenger, 2002).

NO_2 may also indirectly affect air quality and public health by increasing ground-level ozone (O_3), a secondary pollutant formed from the reaction of NO_2 with other precursor compounds emitted by human industrial activity (Tu et al., 2007). Ozone has been identified as one of the two most damaging air pollutants to human health (Miranda et al., 2011; Hajat et al., 2015; Kelly and Fussell, 2015), and also one of the most prevalent outdoor air pollutants in urban areas, making it of great importance for urban public health (D'Amato et al., 2010). The relationship of fossil fuel emissions and air quality is further complicated because the presence of NO may decrease already present O_3 by oxidizing it to NO_2, so areas of high vehicle traffic may have lower levels of O_3 and higher levels of NO_2 depending on the dynamics of NO and NO_2 in the atmosphere (Fenger, 2002). In the future, this dynamic might change further as climate change increasingly pushes air temperatures in urban areas beyond historic norms to new extremes. Specifically, climate change may spur higher formation rates of O_3, increasing the frequency of high O_3 "events" in which levels rapidly accumulate beyond a hazardous threshold (D'Amato et al., 2010), and also increasing the number of peak heat days that coincides with higher NO_2 levels (Goldberg et al., 2021).

Our study found that NO_2 varies significantly between HOLC grades when considering all 11 sampled Midwestern cities. Overall, the greatest difference in NO_2 appears

Downloaded from http://online.ucpress.edu/elementa/article-pdf/10/1/00027/735603/elementa.2022.00027.pdf by guest on 15 August 2022

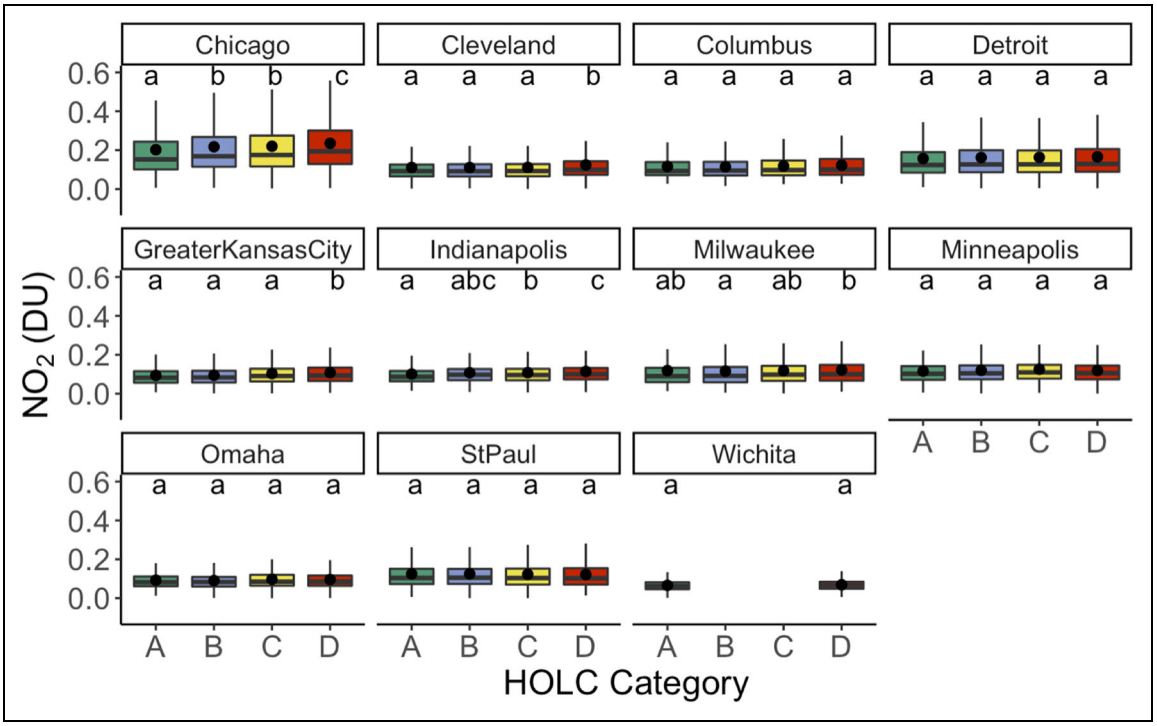

Figure 2. Nitrogen dioxide levels by HOLC neighborhood for 11 Midwestern cities. NO_2 levels, reported in Dobson Units (DU), sampled from HOLC-graded neighborhoods (A–D) were assessed by analysis of variance (ANOVA) considering each city separately. The HOLC, or Home Owner's Loan Commission, assessed urban neighborhoods in the early 20th century for financial "risk." Sample sizes of neighborhood grades for all cities are summarized in Table S3. Lower-case letter notation above boxplots indicate significance according to $P < 0.05$; please see **Figure 1** for explanation of alphabetical notation. Boxplots show the mean (black point), median (horizontal line within box), the 25th and 75th percentiles of the data (upper and lower hinges of the box), and the largest and smallest values within 1.5 times the interquartile range above the 75th and below the 25th percentiles (whiskers extending from box), respectively, for each HOLC-graded neighborhood.

Table 3. Model parameters for mixed-effect models describing the relationship of NO_2 with coarse demographic and geographic variables

Model	Slope ($\pm SD$)	Intercept ($\pm SD$)	R^2
$\sim Area + (1\|City) + \varepsilon$	$8.8 \times 10^{-6} \pm 2.8 \times 10^{-4}$	-2.3 ± 0.15	0.0000163
$\sim PopDens + (1\|City) + \varepsilon$	$5.9 \times 10^{-5} \pm 2.0 \times 10^{-5}$	-2.6 ± 0.11	0.0981
$\sim Pop + (1\|City) + \varepsilon$	$3.0 \times 10^{-7} \pm 8.7 \times 10^{-8}$	-2.5 ± 0.087	0.143

Values presented show each model of individual and combined variables, including area as of 2019 (*Area*, km^2), population density as of 2010 (*PopDens*, people mi^{-2}), and population size as of 2019 (*Pop*, number of people) according to the U.S. Census Bureau. City was included in these mixed-models as a random effect ($1|City$). Models were assessed by R^2 values.

between D-grade neighborhoods with the highest values and A-grade neighborhoods with the lowest, and this variation translates to a mean increase of +7.3% among cities. Chicago exhibited the highest overall levels of NO_2 compared with all other cities, potentially attributable to its large population and congested vehicle traffic. Kerr et al. (2021) demonstrate disproportionately higher burdens of high NO_2 due to vehicle traffic in non-white and low-income neighborhoods—demographic factors which are often represented in redlined areas—even during the periods of COVID-19 lockdowns, when traffic was greatly reduced overall. We also observed a general trend that cities with significant differences in NO_2 between A- and D-grade neighborhoods tended to have the proportion of neighborhoods strongly skewed toward C and D grades, with around 70%–90% of the HOLC designated city area given a C or D grade. Though, Detroit and Wichita also have a similar neighborhood skew, but do not exhibit significant differences in NO_2. It may be that cities that were comprised of more C and D neighborhoods were subject to different development and investment/divestment patterns than the other Midwestern cities, including more extreme industrialization and intracity highway construction, or already contained more C and D

Downloaded from http://online.ucpress.edu/elementa/article-pdf/10/1/00027/735603/elementa.2022.00027.pdf by guest on 15 August 2022

neighborhoods due to preexisting industry and/or existing demographics (Rothstein, 2017). We encourage city-specific multidisciplinary research to examine the drivers and causes of NO_2 in the past, now, and into the future to more completely address these issues.

When we evaluated each city individually, comparing NO_2 across HOLC grades, we found D neighborhoods to have the highest levels of NO_2 in cities that exhibited significant variation across grades. In Chicago, the NO_2 is 16% greater in D neighborhoods compared to A neighborhoods. NO_2 is greater in D neighborhoods by over 10% in 4 out of 5 cities which showed significant differences (Chicago, Indianapolis, Greater Kansas City, and Cleveland). Differences of above 10% for 4 of the 11 cities—as high as 16% for Chicago—are not marginal shifts, especially considering this is an analysis of a single year, 2019, nearly a century after neighborhoods were categorized by the HOLC, and over 50 years after the Fair Housing Act. These data provide evidence that D neighborhoods in large Midwestern cities experience a larger burden of NO_2 pollution than A neighborhoods, demonstrating a modern legacy of redlining and associated inequities that is observed in persistently unequal air quality. Previous studies also support the ability of TROPOMI-derived NO_2 air pollution data to detect differences at high spatial resolutions (Goldberg et al., 2019; Demetillo et al., 2020; Kerr et al., 2021). Demetillo et al. (2020) emphasizes that TROPOMI data can accurately estimate relative differences in ground-level NO_2 values, but may not precisely determine absolute values of NO_2. We suggest our results be used to identify persistent areas of air quality inequality, and encourage higher resolution ground-based data be obtained to quantify absolute values and describe and predict individual and community health impacts. It is important to note that a lack of significant differences NO_2 as estimated by TROPOMI among HOLC neighborhoods does *not* necessarily imply equity in air quality on the ground; we strongly encourage ground-based monitoring to more accurately reveal absolute variation experienced by residents.

Detectable from space, NO_2 pollution poses an uneven public health threat in neighborhoods also facing higher temperatures under climate change due to a mix of increased impervious surface area and lower greenspace (Demetillo et al., 2020; Hoffman et al., 2020; Moxley and Fischer, 2020; Namin et al., 2020). Trees and other vegetation can directly reduce atmospheric NO_2 by uptaking and metabolizing NO_2 molecules through their leaf stomata (Nowak et al., 2014; Grote et al., 2016). On average, urban trees can reduce NO_2 levels by 15% (Rao et al., 2014). Grade A neighborhoods can have as much as 25% more tree canopy cover than D neighborhoods, and this may directly contribute to lower NO_2 values (Locke et al., 2021). These trends taken together emphasize the need for increased tree canopy cover in historically redlined neighborhoods to reduce NO_2 pollution as well as decrease land surface temperatures (Hoffman et al., 2020). However, there are documented issues with relying on tree planting alone to improve air quality, as trees can also contribute to increased pollen and the production of biogenic volatile organic compounds that can lead to ozone (Eisenman et al., 2019). NO_2 is also directly connected with fossil fuel combustion, particularly in industry and transportation (Chen et al., 2007; Goldberg et al., 2019); D-grade neighborhoods frequently have more and denser highways and factories due to selective planning and policies to expand these developments in the D-grade areas (Rothstein, 2017; Bullock et al., 2018; Demetillo et al., 2020; Moxley and Fischer, 2020).

Influence of city characteristics on pollutant levels

Population and population density often correlate with increases in traffic and other sources of fossil fuel emissions, and therefore may be predictive of NO_2 levels (Ou et al., 2016; Goldberg et al., 2021). Our results showing potential relationships between any of the coarse urban geographic variables support the need for higher spatial resolution measurements to detect predictive trends and establish effective working models for understanding urban air quality and how it varies within and across cities (Lamsal et al., 2013; Zhu et al., 2014). While satellite sensing is a powerful tool, the resolution discrepancies in urban areas demand that ground-based sensor networks be installed to fully understand the nuances of each region and what controls these pollutants within and across redlined neighborhoods so we can work effectively toward environmental justice in these cities.

Future directions and conclusions

We demonstrate the potential of TROPOMI-collected data for monitoring and evaluating NO_2 air pollution across neighborhoods in cities historically categorized by HOLC grades in the U.S. Midwest. This is an advancement in monitoring air quality in the United States and globally since ground-based sensors within an area are often limited by number, spatial distribution, or by the frequency of temporal data collection. These methods can and should be applied to additional cities representing different climates, biomes, population densities, and development histories, as well as those impacted differently from current and projected climate change. Exploring the industrial, economic, and social histories of individual cities, including the ones we focused on in this study, will also allow for the understanding of historical drivers of observed inequalities.

TROPOMI collects data on other air pollutants, including CO and O_3, both of which are listed in the EPA's 6 Criteria Air Pollutants. Current coarseness of those data—assessment of the total rather than tropospheric atmospheric column in the former, and pixels of very large size in the latter—prevent using them from accurately estimating local, ground-level concentrations. As satellite detecting capabilities become even higher resolution, these and other pollutants can be tracked by similar monitoring methods. Our study also applied an area-based cutoff to better align with NO_2 pixel size and minimize oversampling issues; however, this approach limits understanding more about the presence and impact of potential isolated, high-emissions neighborhoods that could strongly affect residents' health. To better incorporate data

Downloaded from http://online.ucpress.edu/elementa/article-pdf/10/1/00027/735603/elementa.2022.00027.pdf by guest on 15 August 2022

from these smaller neighborhoods and to effectively scale from ground to satellite, we suggest further exploration of high-resolution ground-based sensor networks that consider HOLC neighborhood histories for future investigations. The Pandonia Global Network (http://pandonia-global-network.org), a ground-based sensor network used to ground-truth tropospheric data collected from satellites, is an active and extremely promising initiative to further understand how to collect accurate, real-time, open-data on air pollutants that are important to human health (Judd et al., 2020; Verhoelst et al., 2021). However, the distribution and locations of these sensors is not ubiquitous, and not yet useful for within-city comparisons in the U.S. Midwest (Judd et al., 2020; Verhoelst et al., 2021).

We also encourage examining variation across seasons and day of week, as patterns and type of human activities may vary significantly, and temperature changes across seasons—particularly in the seasonal Midwest—may influence the chemistry of the formation of these compounds in the air (Goldberg et al., 2021). Further, assessing interannual variations and patterns may inform predictions of the long-term influence of climate change on urban air pollution. Finally, employing oversampling methods within the HOLC neighborhood polygons could allow for greater signal-to-noise ratios in the TROPOMI data (Lamsal et al., 2013; Zhu et al., 2014).

Despite variation in the development history, size and economy between the 11 large Midwestern cities, there is a consistent pattern of higher NO_2 in D-grade neighborhoods based on our study using satellite data collected for the calendar year of 2019. This is strong evidence of a legacy of environmental inequalities tied to the policy of federally commissioned redlining that persisted under decades of political marginalization and systemic racism (Rothstein, 2017). While we did not directly investigate the composition of the demographic data, it is likely D-grade neighborhoods are still primarily comprised of low-income residents and residents of color, since this pattern is seen in many cities today (Mitchell and Franco, 2018). Recent research that integrates demographic data with air quality data shows that pollution burdens in historically redlined neighborhoods fall disproportionately on Black and Hispanic residents (Demetillo et al., 2020; Kerr et al., 2021; Gonzalez et al., 2022; Lane et al., 2022) and are likely to influence the health of these residents (Nardone et al., 2020b; Nardone et al., 2020c; Anenberg et al., 2022). These relationships support the responsibility of city, state, and federal governments to rectify these historic and present-day inequalities and harms. Our results warrant further research identifying the specific sources and causes of concentrated air pollution within individual cities that contribute to modern day inequalities, which can then be targeted by government policies, and reparations for residents, a practice which is gaining traction at local levels (Brown et al., 2021). Based on our findings, we suggest future research look toward establishing high-temporal resolution sensors on residences, schools, and in public spaces in cities historically categorized by the HOLC, which would be key to understanding pollution burden on urban residents and addressing these burdens through public health support, city planning interventions, and financial reparations.

Data accessibility statement

The following datasets were generated for our study and are openly available:

Hrycyna, Elizabeth; Mergenthal, Jennings G.A.; Noor, Saiido; Heskel, Mary A. 2022. Satellite observations of NO_2 indicate legacy impacts of redlining in U.S. Midwestern cities. Available at https://doi.org/10.5281/zenodo.6536071.

Supplemental files

The supplemental files for this article can be found as follows:

Tables S1–S3. Docx

Acknowledgments

We would like to acknowledge Profs. Mary Montgomery of Macalester College and Sarah Fortner of the Science Education Resource Center of Carleton College for their roles in providing feedback as senior honors thesis committee members. We also deeply appreciate Macalester College for funding the collaborative summer undergraduate research fellowship and Wallace Fund faculty research grant support that led to this study. Publication of this article was funded by the Macalester College Dewitt Wallace Library Open Access Fund. Finally, we thank the creators of *Mapping Inequality* for making shapefile data openly available and sparking so many needed conversations and studies about redlining.

Competing interests

We, as an author group, have no competing interests to declare.

Author contributions

- Contributed to conception and design: EH, MAH.
- Contributed to acquisition of data: EH, SN, MAH.
- Contributed to analysis and interpretation of data: EH, MAH, SN, JGAM.
- Drafted and/or revised the article: EH, JGAM, SN, MAH.
- Final approval of the version to be published: EH, JGAM, SN, MAH.

References

Anenberg, SC, **Mohegh, A**, **Goldberg DL**, **Kerr, GH**, **Brauer, M**, **Burkart, K**, **Hystad, P**, **Larkin, A**, **Wozniak, S**, **Lamsal, L.** 2022. Long-term trends in urban NO_2 concentrations and associated paediatric asthma incidence: Estimates from global datasets. *The Lancet Planetary Health* **6**(1): e49–e58. DOI: https://dx.doi.org/10.1016/S2542-5196(21)00255-2.

Brown, A, **de Sainte Maresville, E**, **Yang, A.** 2021. How the 1st US city to fund reparations for Black residents is making amends. Available at https://abcnews.go.com/US/1st-us-city-fund-reparations-

Downloaded from http://online.ucpress.edu/elementa/article-pdf/10/1/00027/735603/elementa.2022.00027.pdf by guest on 15 August 2022

black-residents-making/story?id=76118463. Accessed 11 January 2022.

Bullock, C, **Ard, K**, **Saalman, G.** 2018. Measuring the relationship between state environmental justice action and air pollution inequality, 1990-2009. *The Review of Policy Research* **35**(3): 466–490. DOI: https://dx.doi.org/10.1111/ropr.12292.

Champley, S. 2020. *pwr: Basic functions for power analysis*. R package version 1.3-0. Available at https://CRAN.R-project.org/package=pwr. Accessed 11 April 2022.

Chen, T-M, **Gokhale, J**, **Shofer, S**, **Kuschner, WG.** 2007. Outdoor air pollution: Nitrogen dioxide, sulfur dioxide, and carbon monoxide health effects. *The American Journal of the Medical Sciences* **333**(4): 249–256. DOI: https://dx.doi.org/10.1097/MAJ.0b013e31803b900f.

Clark, LP, **Millet, DB**, **Marshall, JD.** 2014. National patterns in environmental injustice and inequality: Outdoor NO_2 air pollution in the United States. *PLoS One* **9**(4): e94431. DOI: https://dx.doi.org/10.1371/journal.pone.0094431.

Clark, MA, **Springmann, M**, **Hill, J**, **Tilman, D.** 2019. Multiple health and environmental impacts of foods. *Proceedings of the National Academy of Sciences of the United States of America* **116**(46): 23357–23362. DOI: https://dx.doi.org/10.1073/pnas.1906908116.

Cooper, MJ, **Martin, RV**, **Hammer, MS**, **Levelt, PF**, **Veefkind, P**, **Lamsal, LN**, **Krotkov, NA**, **Brook, JR**, **McLinden, CA.** 2022. Global fine-scale changes in ambient NO_2 during COVID-19 lockdowns. *Nature* **601**: 380–387. DOI: https://dx.doi.org/10.1038/s41586-021-04229-0.

D'Amato, G, **Cecchi, L**, **D'Amato, M**, **Liccardi G.** 2010. Urban air pollution and climate change as environmental risk factors of respiratory allergy: An update. *Journal of Investigational Allergology & Clinical Immunology* **20**(2): 95–102. Available at https://www.ncbi.nlm.nih.gov/pubmed/20461963.

Demetillo, MAG, **Navarrow, A**, **Knowles, KK**, **Fields, KP**, **Geddes, G**, **Nowlan, C**, **Janz, SJ**, **Judd, LM**, **Al-Saadi, J**, **Sun, K**, **McDonald, BC**, **Diskin, GS**, **Pusede, SE.** 2020. Observing nitrogen dioxide air pollution using high-spatial-resolution remote sensing measurements in Houston, Texas. *Environmental Science and Technology* **54**(16): 9882–9895. DOI: https://dx.doi.org/10.1021/acs.est.0c01864.

Eisenman, TS, **Jariwala, SP**, **Lovasi, GS.** 2019. Urban trees and asthma: A call for epidemiological research. *The Lancet Respiratory Medicine* **7**(7): E19–E20. DOI: https://dx.doi.org/10.1016/s2213-2600(19)30193-6.

Fenger, J. 2002. Urban air quality, in Austin, J, Brimblecombe, P, Sturges, W eds., *Developments in environmental science*. Amsterdam, The Netherlands: Elsevier. DOI: https://dx.doi.org/10.1016/s1474-8177(02)80004-3.

Fishback, PV, **Rose, J**, **Snowden, KA**, **Storrs, T.** 2021. *New evidence on redlining by federal housing programs in the 1930s* [Working Paper 29244]. Cambridge, MA: National Bureau of Economic Research. DOI: https://dx.doi.org/10.3386/w29244.

Goldberg, DL, **Anenberg, SC**, **Kerr, GH**, **Mohegh, A**, **Lu, Z**, **Streets, DG.** 2021. TROPOMI NO_2 in the United States: A detailed look at the annual averages, weekly cycles, effects of temperature, and correlation with surface NO_2 concentrations. *Earth's Future* **9**(4): e2020EF001665. DOI: https://dx.doi.org/10.1029/2020EF001665.

Goldberg, DL, **Lu, Z**, **Streets, DG**, **de Foy, B**, **Griffin, D**, **McLinden, CA**, **Lamsal, LN**, **Krotkov, NA**, **Eskes, H.** 2019. Enhanced capabilities of TROPOMI NO_2: Estimating NOx from North American cities and power plants. *Environmental Science and Technology* **53**(21): 12594–12601. DOI: https://dx.doi.org/10.1021/acs.est.9b04488.

Gonzalez, DJX, **Nardone, A**, **Nguyen, AV**, **Morello-Frosch, R**, **Casey, JA.** 2022. Historic redlining and the siting of oil and gas wells in the United States. *Journal of Exposure Science & Environmental Epidemiology*. DOI: https://dx.doi.org/10.1038/s41370-022-00434-9.

Gorelick, N, **Hancher, M**, **Dixon, M**, **Ilyushchenko, S**, **Thau, D**, **Moore, R.** 2017. Google earth engine: Planetary-scale geospatial analysis for everyone. *Remote Sensing of Environment*. DOI: https://dx.doi.org/10.1016/j.rse.2017.06.031.

Grote, R, **Samson, R**, **Alonso, R**, **Amorim, JH**, **Carinanos, P**, **Churkina, G**, **Fares, S**, **Thiec, DL**, **Niinemets, U**, **Mikkelsen, TN**, **Paoletti, E**, **Tiwary, A**, **Calfapietra, C.** 2016. Functional traits of urban trees: Air pollution mitigation potential. *Frontiers in Ecology and the Environment* **14**(10): 543–550. DOI: https://dx.doi.org/10.1002/fee.1426.

Grove, M, **Ogden, L**, **Pickett, S**, **Boone, C**, **Buckley, G**, **Locke, D**, **Lord, C**, **Hall, B**. 2018. The legacy effect: Understanding how segregation and environmental injustice unfold over time in Baltimore. *Annals of the American Association of Geographers* **108**: 524–537. DOI: https://dx.doi.org/10.1080/24694452.2017.1365585.

Hajat, A, **Hsia, C**, **O'Neill, MS.** 2015. Socioeconomic disparities and air pollution exposure: A global review. *Current Environmental Health Reports* **2**(4): 440–450. DOI: https://dx.doi.org/10.1007/s40572-015-0069-5.

Hill, J, **Goodkind, A**, **Tessum, C**, **Thakrar, S**, **Tilman, D**, **Polasky, S**, **Smith, T**, **Hunt, N**, **Mullins, K**, **Clark, M**, **Marshall, J.** 2019. Air-quality-related health damages of maize. *Nature Sustainability* **2**(5): 397–403. DOI: https://dx.doi.org/10.1038/s41893-019-0261-y.

Hoffman, JS, **Shandas, V**, **Pendleton, N.** 2020. The effects of historical housing policies on resident exposure to intra-urban heat: A study of 108 US urban areas. *Climate* **8**(1): 12. DOI: https://dx.doi.org/10.3390/cli8010012.

Hothorn, T, **Bretz, F**, **Westfall, P.** 2008. Simultaneous inference in general parametric models. *Biometrical Journal* **50**(3): 346–363.

Downloaded from http://online.ucpress.edu/elementa/article-pdf/10/1/00027/735603/elementa.2022.00027.pdf by guest on 15 August 2022

Jing, P, **Goldberg, DL.** 2022. Influence of conducive weather on ozone in the presence of reduced NOx emissions: A case study in Chicago during the 2020 lockdowns. *Atmospheric Pollution Research* **13**(2): 101313. DOI: https://dx.doi.org/10.1016/j.apr.2021.101313.

Judd, LM, **Al-Saadi, JA**, **Szykman, JJ**, **Valin, LC**, **Janz, SJ**, **Kowalewski, MG**, **Eskes, HJ**, **Veefkind, JP**, **Cede, A**, **Mueller, M**, **Gebetsberger, M**, **Swap, R**, **Pierce, RB**, **Nowlan, CR**, **Abad, GG**, **Nehrir, A**, **Williams, D.** 2020. Evaluating sentinel-5P TROPOMI tropospheric NO_2 column densities with airborne and Pandora spectrometers near New York City and Long Island Sound. *Atmospheric Measurement and Technology* **13**(11): 6113–6140. DOI: https://dx.doi.org/10.5194/amt-13-6113-2020.

Kelly, FJ, **Fussell, JC.** 2015. Air pollution and public health: Emerging hazards and improved understanding of risk. *Environmental Geochemistry and Health* **37**(4): 631–649. DOI: https://dx.doi.org/10.1007/s10653-015-9720-1.

Kerr, GH, **Goldberg, DL**, **Anenberg, S.** 2021. COVID-19 pandemic reveals persistent disparities in nitrogen dioxide pollution. *Proceedings of the National Academy of Sciences* **118**(30): e2022409118. DOI: https://dx.doi.org/10.1073/pnas.2022409118.

Krieger, N, **Van Wye, G**, **Huynh, M**, **Waterman, PD**, **Maduro, G**, **Li, W**, **Gwynn, RC**, **Barbot, O**, **Bassett, MT.** 2020a. Structural racism, historical redlining, and risk of preterm birth in New York City, 2013-2017. *American Journal of Public Health* **110**(7): 1046–1053. DOI: https://dx.doi.org/10.2105/AJPH.2020.305656.

Krieger, N, **Wright, E**, **Chen, JT**, **Waterman, PD**, **Huntley, ER**, **Arcaya, M.** 2020b. Cancer stage at diagnosis, historical redlining, and current neighborhood characteristics: Breast, cervical, lung, and colorectal cancers, Massachusetts, 2001–2015. *American Journal of Epidemiology* **189**(10): 1065–1075. DOI: https://dx.doi.org/10.1093/aje/kwaa045.

Lamsal, LN, **Martin, RV**, **Parrish, DD**, **Krotkov, NA.** 2013. Scaling relationship for NO_2 pollution and urban population size: A satellite perspective. *Environmental Science and Technology* **47**(14): 7855–7861. DOI: https://dx.doi.org/10.1021/es400744g.

Lane, HM, **Morello-Frosch, R**, **Marshall, JD**, **Apte, J.** 2022. Historical redlining is associated with present-day air pollution disparities in U.S. cities. *Environmental Science Technology Letters* **9**(4): 345–350. DOI: https://dx.doi.org/10.1021/acs.estlett.1c1012.

Le Quéré, C, **Jackson, RB**, **Jones, MW**, **Smith, AJP**, **Abernethy, S**, **Andrew, RM**, **De-Gol, AJ**, **Willis, DR**, **Shan, Y**, **Canadell, JG**, **Friedlingstein, P**, **Creutzig, F**, **Peters, GP.** 2020. Temporary reduction in daily global CO2 emissions during the COVID-19 forced confinement. *Nature Climate Change* **10**(7): 647–653. DOI: https://dx.doi.org/10.1038/s41558-020-0797-x.

Lenth, RV. 2022. *emmeans: Estimated marginal means, aka least-squares means*. R package version 1.7.2. Available at https://cran.r-project.org/package=emmeans. Accessed 11 April 2022.

Li, D, **Newman, GD**, **Wilson, B**, **Zhang, Y**, **Brown, RD.** 2021. Modeling the relationships between historical redlining, urban heat, and heat-related emergency department visits: An examination of 11 Texas cities. *Environment and Planning B: Urban Analytics and City Science*. DOI: https://dx.doi.org/10.1177/23998083211039854.

Liu, J, **Clark, LP**, **Bechle, MJ**, **Hajat, A**, **Kim, SY**, **Robinson, AL**, **Sheppard, L**, **Szpiro, AA**, **Marshall, JD.** 2021. Disparities in air pollution exposure in the United States by race/ethnicity and income, 1990-2010. *Environmental Health Perspectives* **129**(12): 127005. DOI: https://dx.doi.org/10.1289/EHP8584.

Locke, DH, **Hall, B**, **Grove, JM**, **Pickett, STA**, **Ogden, LA**, **Aoki, C**, **Boone, CG**, **O'Neil-Dunne, JPM.** 2021. Residential housing segregation and urban tree canopy in 37 US Cities. *NPJ Urban Sustainability* **1**(1): 1–9. DOI: https://dx.doi.org/10.1038/s42949-021-00022-0.

Miranda, ML, **Edwards, SE**, **Keating, MH**, **Paul, CJ.** 2011. Making the environmental justice grade: The relative burden of air pollution exposure in the United States. *International Journal of Environmental Research and Public Health* **8**(6): 1755–1771. DOI: https://dx.doi.org/10.3390/ijerph8061755.

Mitchell, B, **Franco, J.** 2018. HOLC 'redlining' maps: The persistent structure of segregation and economic inequality. Washington, DC. Available at https://dataspace.princeton.edu/handle/88435/dsp01dj52w776n. Accessed 20 December, 2021.

Morello-Frosch, R, **Jesdale, BM.** 2006. Separate and unequal: Residential segregation and estimated cancer risks associated with ambient air toxics in U.S. metropolitan areas. *Environmental Health Perspectives* **114**(3): 386–393. DOI: https://dx.doi.org/10.1289/ehp.8500.

Moxley, D, **Fischer, B.** 2020. Historic HOLC redlining in Indianapolis and the legacy of environmental impacts. *Journal of Public and Environmental Affairs* **1**(1). DOI: https://dx.doi.org/10.14434/jpea.v1i1.30321.

Namin, S, **Xu, W**, **Zhou, Y**, **Beyer, KMM.** 2020. The legacy of the Home Owners' Loan Corporation and the political ecology of urban trees and air pollution in the United States. *Social Science & Medicine* **246**: 112758. DOI: https://dx.doi.org/10.1016/j.socscimed.2019.112758.

Nardone, A, **Casey, JA**, **Morello-Frosch, R**, **Mujahid, M**, **Balmes, JR**, **Thakur, N.** 2020a. Associations between historical residential redlining and current age-adjusted rates of emergency department visits due to asthma across eight cities in California: An ecological study. *The Lancet Planetary Health*. DOI: https://dx.doi.org/10.1016/s2542-5196(19)30241-4.

Nardone, A, **Chiang, J**, **Corburn, J.** 2020b. Historic redlining and urban health today in U.S. cities. *Environmental Justice* **13**(4): 109–119. DOI: https://dx.doi.org/10.1089/env.2020.0011.

Downloaded from http://online.ucpress.edu/elementa/article-pdf/10/1/00027/735603/elementa.2022.00027.pdf by guest on 15 August 2022

Nardone, AL, **Casey, JA**, **Rudolph, KE**, **Karasek, D**, **Mujahid, M**, **Morello-Frosch, R.** 2020c. Associations between historical redlining and birth outcomes from 2006 through 2015 in California. *PLoS One* **15**(8): e0237241. DOI: https://dx.doi.org/10.1371/journal.pone.0237241.

Nelson, RK, **Winling, L**, **Marciano, R**, **Connolly, N.** 2021. Mapping inequality: Redlining in New Deal America. Available at https://dsl.richmond.edu/panorama/redlining/. Accessed 20 January 2021.

Nowak, DJ, **Hirabayashi, S**, **Bodine, A**, **Greenfield, EJ.** 2014. Tree and forest effects on air quality and human health in the United States. *Environmental Pollution* **193**: 119–129. DOI: https://dx.doi.org/10.1016/j.envpol.2014.05.028.

Ou, J, **Liu, X**, **Li, X**, **Shi, X.** 2016. Mapping global fossil fuel combustion CO_2 emissions at high resolution by integrating nightlight, population density, and traffic network data. *IEEE Journal of Selected Topics in Applied Earth Observations and Remote Sensing* **9**(4): 1674–1684. DOI: https://dx.doi.org/10.1109/JSTARS.2015.2476347.

Park, KA, **Quercia, RG.** 2020. Who lends beyond the red line?The community reinvestment act and the legacy of redlining. *Housing Policy Debate*. Available at https://www.tandfonline.com/doi/abs/10.1080/10511482.2019.1665839.

R Core Team. 2021. *R: A language and environment for statistical computing*. Vienna, Austria: R Foundation for Statistical Computing. Available at https://www.R-project.org/.

Rao, M, **George, LA**, **Rosenstiel, TN**, **Shandas, V**, **Dinno, A.** 2014. Assessing the relationship among urban trees, nitrogen dioxide, and respiratory health. *Environmental pollution* **194**: 96–104. DOI: https://dx.doi.org/10.1016/j.envpol.2014.07.011.

Rothstein, R. 2017. *The color of law: A forgotten history of how our government segregated America*. New York, NY: Liveright Publishing.

Rumchev, K, **Brown, H**, **Spickett, J.** 2007. Volatile organic compounds: Do they present a risk to our health? *Reviews on Environmental Health* **22**(1): 39–55. DOI: https://dx.doi.org/10.1515/reveh.2007.22.1.39.

Tessum, CW, **Apte, JS**, **Goodkind, AL**, **Muller, NZ**, **Mullins, KA**, **Paolella, DA**, **Polasky, S**, **Springer, NP**, **Thakrar, SK**, **Marshall, JD**, **Hill, JD.** 2019. Inequity in consumption of goods and services adds to racial-ethnic disparities in air pollution exposure. *Proceedings of the National Academy of Sciences* **116**(13): 6001–6006. DOI: https://dx.doi.org/10.1073/pnas.1818859116.

Tessum, CW, **Paolella, DA**, **Chambliss, SE**, **Apte, JS**, **Hill, JD**, **Marshall, JD.** 2021. $PM_{2.5}$ polluters disproportionately and systemically affect people of color in the United States. *Science Advances* **7**(18): eabf4491. DOI: https://dx.doi.org/10.1126/sciadv.abf4491.

Tu, J, **Xia, Z-G**, **Wang, H**, **Li, W.** 2007. Temporal variations in surface ozone and its precursors and meteorological effects at an urban site in China. *Atmospheric Research* **85**(3): 310–337. DOI: https://dx.doi.org/10.1016/j.atmosres.2007.02.003.

Tzortziou, M, **Kwong, CF**, **Goldberg, D**, **Schiferl, L**, **Commane, R**, **Abuhassan, N**, **Szykman, JJ**, **Valin, LC.** 2022. Declines and peaks in NO_2 pollution during multiple waves of the COVID-10 pandemic in the New York metropolitan area. *Atmospheric Chemistry and Physics* **22**: 2399–2417. DOI: https://dx.doi.org/10.5194/acp-22-2399-2022.

Verhoelst, T, **Compernolle, S**, **Pinardi, G**, **Lambert, JC**, **Eskes, H**, **Eichmann, KU**, **Fjaeraa, AM**, **Granville, J**, **Niemeijer, S**, **Cede, A**, **Tiefengraber, M**, **Hendrick, F**, **Pazmiño, A**, **Bais, A**, **Bazureau, A**, **Boersma, KF**, **Bognar, K**, **Dehn, A**, **Donner, S**, **Elokhov, A**, **Gebetsberger, M**, **Goutail, F**, **Grutter, M**, **Gruzdev, AN**, **Gratsea, M**, **Hansen, G**, **Irie, H**, **Jepsen, N**, **Kanaya, Y**, **Karagkiozidis, D**, **Kivi, R**, **Kreher, K**, **Levelt, PF**, **Liu, C**, **Mueller, M**, **Navarro-Comas, M**, **Piters, AJM**, **Pommereau, JP**, **Portafaix, T**, **Prados-Roman, C**, **Puentedura, O**, **Querel, R**, **Remmers, J**, **Richter, A**, **Rimmer, J**, **Cárdenas, CR**, **de Miguel, LS**, **Sinyakov, VP**, **Stremme, W**, **Strong, K**, **Van Roozendael, M**, **Veefkind, JP**, **Wagner, T**, **Wittrock, F**, **Yela, M**, **Zehner, C.** 2021. Ground-based validation of the Copernicus Sentinel-5P TROPOMI NO_2 measurements with the NDACC ZSL-DOAS, MAX-DOAS and Pandonia global networks. *Atmospheric Measurement Techniques* **14**: 481–510. DOI: https://dx.doi.org/10.5194/amt-14-481-2021.

Wickham, H. 2021. *tidyr: Tidy messy data*. R package version 1.1.3. Available at https://cran.r-project.org/package=tidyr. Accessed 20 January 2021.

Wilson, B. 2020. Urban heat management and the legacy of redlining. *Journal of the American Planning Association* **86**(4): 443–457. DOI: https://dx.doi.org/10.1080/01944363.2020.1759127.

Winling, LC, **Michney, TM.** 2021. The roots of redlining: Academic, governmental, and professional networks in the making of the new deal lending regime. *Journal of American History* **108**(1): 42–69. DOI: https://dx.doi.org/10.1093/jahist/jaab066.

Woods, LL. 2012. The federal home loan bank board, redlining, and the national proliferation of racial lending discrimination, 1921–1950. *Journal of Urban History* **38**(6): 1036–1059. DOI: https://dx.doi.org/10.1177/0096144211435126.

Zenou, Y, **Boccard, N.** 2000. Racial discrimination and redlining in cities. *Journal of Urban Economics* **48**(2): 260–285. DOI: https://dx.doi.org/10.1006/juec.1999.2166.

Zhu, L, **Jacob, DJ**, **Mickley, LJ**, **Marais, EA**, **Cohan, D**, **Yoshida, Y**, **Duncan, B**, **Abad, GG**, **Chance, KV.** 2014. Anthropogenic emissions of highly reactive volatile organic compounds in eastern Texas inferred from oversampling of satellite (OMI) measurements of HCHO columns. *Environmental Research Letters* **9**: 114004. DOI: https://dx.doi.org/10.1088/1748-9326.

Downloaded from http://online.ucpress.edu/elementa/article-pdf/10/1/00027/735603/elementa.2022.00027.pdf by guest on 15 August 2022

Downloaded from http://online.ucpress.edu/elementa/article-pdf/10/1/00027/735603/elementa.2022.00027.pdf by guest on 15 August 2022

How to cite this article: Hrycyna, E, Mergenthal, JGA, Noor, S, Heskel, MA. 2022. Satellite observations of NO_2 indicate legacy impacts of redlining in U.S. Midwestern cities. *Elementa: Science of the Anthropocene* 10(1). DOI: https://doi.org/10.1525/elementa.2022.00027

Domain Editor-in-Chief: Detlev Helmig, Boulder AIR LLC, Boulder, CO, USA

Associate Editor: Maria Val Martin, School of Biosciences, The University of Sheffield, Sheffield, UK

Knowledge Domain: Atmospheric Science

Published: July 29, 2022 **Accepted:** June 23, 2022 **Submitted:** February 9, 2022

Copyright: © 2022 The Author(s). This is an open-access article distributed under the terms of the Creative Commons Attribution 4.0 International License (CC-BY 4.0), which permits unrestricted use, distribution, and reproduction in any medium, provided the original author and source are credited. See http://creativecommons.org/licenses/by/4.0/.

ELEMENTA Science of the Anthropocene

Elem Sci Anth is a peer-reviewed open access journal published by University of California Press.

OPEN ACCESS